Vol. 5(16) Jul. 2015, PP. 2313-2326

Contents list available at IJMEC

International Journal of Mechatronics, Electrical and Computer Technology (IJMEC)

Journal Homepage: www.aeuso.org

PISSN: 2411-6173 - EISSN: 2305-0543

Controlling the Depth of Anesthesia Using Adaptive Fuzzy Sliding Mode Control Strategy

Seyyed Hossein Sadat Hosseini[1], Mohammad Khazaei[1*], Ziba Asadnejad Khomarlou[1], and Amir Hossein Geramipour[2]

[1]*Electrical and Computer Engineering, Iran University of Science and Technology*

[2]*Electrical and Computer Engineering, Amirkabir University of Technology*

***Corresponding Author's E-mail:** m.khazaei1368@gmail.com*

Abstract

A Major impediment to developing a control methodology for controlling the depth of anesthesia (DOA) is the design of a robust control strategy which provides precise input tracking, to be robust versus inter-intra patient's variability and external disturbances. In this study, we proposed a new robust strategy which incorporates an auto-tuning neuron into the adaptive fuzzy sliding mode control (AFSMC) for controlling the DOA. In this study fuzzy systems are applied to approximate the system uncertainties. The main obstacle of conventional sliding mode control is chattering problem. To address this problem, we combined AFSMC with neural control. AFSMC acts as a main controller and forces the system state toward the sliding surface. Neural controller acts as an axillary controller and when the state of the system closes into the boundary layer, AFSMC is replaced by the neural controller. The stability study of the proposed strategy is performed by using the Lyapunov stability theory. Pharmacokinetic-Pharmacodynamic model has been used as a model of patients. Control performance of AFSMC strategy has been compared with fuzzy logic controller (FLC). Simulation results on 8 patients show that the proposed approach achieves a reliable controller with accurate tracking of input signal in the presence of patient variability and external disturbance. Compared to previous studies our proposed strategy has several advantages such as shorter settling time, elimination of overdosing and under dosing, and generating a smooth control input signal without intense switching action.

Keywords: *Adaptive fuzzy sliding mode control (AFSMC), depth of anesthesia (DOA), neural controller, pharmacokinetic-pharmacodynamic model.*

1. Introduction

General anesthesia is a medically induced coma which is commonly produced by a combination of intravenous drugs and inhaled gasses. Another definition for general anesthesia is the lack of responses to noxious stimuli [1]. This procedure consists of three components: muscle relaxation, analgesia, and unconsciousness [2]. Propofol is an intravenously administered anesthetic drug with no analgesic properties that is used in combination with remifentanil to induce and maintain anesthesia during surgery [3], [4]. There are several biological indexes in clinical practice that anesthesiologist use them for determining the DOA such as blood pressure, heart rate, pupil response, and movement [5]. Although for control applications, a measureable index must be used, many of these indexes are not measureable and available in clinical environments. One of the most commonly indexes which uses processed electroencephalogram signals to measure the effects of

Article History:

Received Date: Mar. 01, 2015

Accepted Date: Jun. 25, 2015

Available Online: Jul. 07, 2015

anesthetics and sedatives on the brain, is bispectral index (BIS). The value of BIS is located between the ranges of 0 to 100 (0, coma; 40 to 60, general anesthesia; 60 to 90, sedated; 100, awake) [3]. For closed-loop control of anesthesia, BIS is better than other indexes because of its availability in operating rooms [6]. Closed-loop control has a wide variety of applications in biomedical engineering and modern medicine such as robotic surgery, electrophysiological systems, life support, and image-guided therapy and surgery [6]. One of its applications is drug delivery such as insulin delivery in diabetic patients and propofol delivery in general anesthesia. In this area, closed-loop control plays an important role because improper dosing may cause increasing the risks and costs. For instance, injection of anesthetic drug needs to be adjusted in order to avoid both underdosing and overdosing [6]. Underdosing may cause pain and awareness during surgery, whereas overdosing may cause a delayed recovery, respiratory, and cardiovascular collapse [7].

Many conventional controllers were used for controlling the DOA such as P, PI, and PID [8], [9]. These controllers are simple but do not have good performance in the presence of inter-intra patient's variability and disturbances. Genetic fuzzy controllers, fuzzy controllers, and self-organizing fuzzy controllers were also used [10]-[12]. In order to compensate the effects of uncertainty and disturbances, it is necessary to use adaptive and robust control approaches such as model predictive control (MPC), neural control, sliding mode control (SMC) [13-15] and etc. Van Heusden *et al.* developed a robust PID controller with high accuracy for propofol infusion in children age 6–17 [16]. Because the anesthesia is a nonlinear process and contains a time delay, researchers in [3], [7], [5] employed model predictive controllers (MPCs) to achieve an appropriate DOA level without compromising the patient's health, while the input and output variables were respectively propofol and BIS. In [17], a robust deadbeat control technique with short settling time and robust to disturbances caused by parameter changes was proposed.

In this direction, some other control strategies such as internal model control (IMC), adaptive control using a simple regression model, and H_∞, respectively were taken into account as well [18]-[20]. Finally, high-order SMC was used to maintain the optimal level of anesthesia where the controller had a good performance despite inter-intra patient's variability [21].

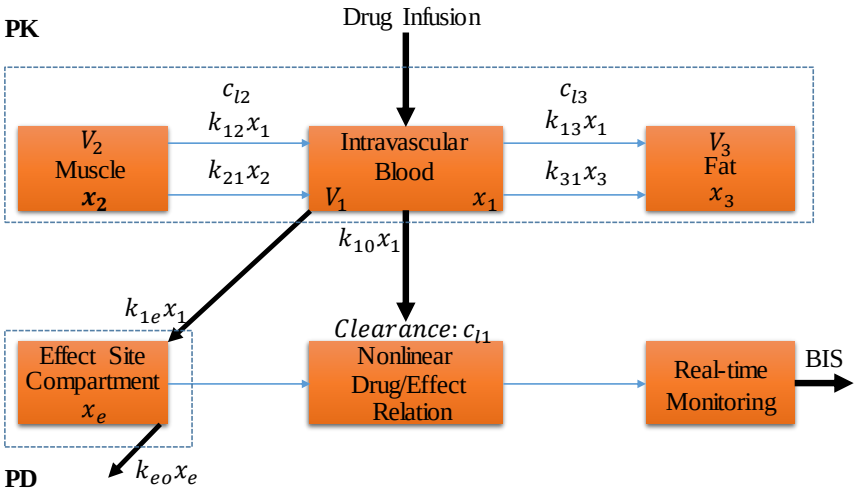

Figure 1: Compartmental model of the patient, where PK denotes the pharmacokinetic model and PD denotes the pharmacodynamic model [4].

Because of insufficient information about system or purposeful mathematical simplification, discrepancies may occur between the actual plant and the mathematical model developed for the controller design. To deal with these discrepancies a robust control method which is known as SMC

has been developed and reported in literature [22]-[27]. Inter-intra patient's variability, external disturbances, underdosing and overdosing are the main problems of controlling the DOA. In order to address these problems, we have proposed a novel robust technique which incorporates an auto-tuning neuron into AFSMC. Pharmacokinetic-Pharmacodynamic model has been used as a model of patients. Simulation results show accurate tracking of input signals without underdosing and overdosing in the presence of patient variability and external disturbance. Compared to previous studies our proposed strategy has several advantages such as shorter settling time, elimination of overdosing and underdosing, and generating a smooth control input signal without intense switching action.

The organization of the paper is as follows. The patient model is described in section 2. In section 3, controller design technique is introduced to design the AFSMC controller. The results are provided in section 4 and section 5 concludes the paper.

2. Patient model

To describe the relationship between the drug infusion rate and its effect, pharmacokinetic-pharmacodynamic model has been used in a way that Pharmacokinetic and pharmacodynamic models explain the distribution of the drug in the body and the relationship between blood concentration of a drug and its clinical effect, respectively. The pharmacokinetic model can be presented by a three-compartment model (see Figure 1). In this model central compartment contains the arterial blood and other tissues such as liver and brain, second compartment includes muscles and viscera, and third compartment contains fat and bones [3]. The mathematical expressions governing this model can be obtained by following equations [4]:

$$\begin{bmatrix} \dot{x}_1(t) \\ \dot{x}_2(t) \\ \dot{x}_3(t) \end{bmatrix} = \begin{bmatrix} -(k_{10}+k_{12}+k_{13}) & k_{21} & k_{31} \\ k_{12} & -k_{21} & 0 \\ k_{13} & 0 & -k_{31} \end{bmatrix} \begin{bmatrix} x_1(t) \\ x_2(t) \\ x_3(t) \end{bmatrix} + \begin{bmatrix} 1 \\ 0 \\ 0 \end{bmatrix} u(t) . \quad (1)$$

Where, $x_1(t)$, $x_2(t)$ and $x_3(t)$ denote the amount of the drug in central, second and third compartments, respectively. The constant k_{10} is the rate of drug metabolism. The constants k_{ji} with $j \neq i$ represent the drug amount transfer rate of drug from jth compartment to ith compartment and $u(t)$ is the infusion rate of the drug (propofol) into the central compartment. Drug concentration of each compartment can be obtained by division of amount of drug on that compartment to related volume of that compartment. One of the most popular models for propofol is Schnider model [29], which calculates the constants as equation (2), in which the Lean Body Mass (LBM) for men and women can be calculated as equation (3) and equation (4), respectively.

$$V_1 = 4.27\,[l], V_2 = 1.89 - 0.3914\,(age - 53)\,[l], V_3 = 238\,[l]$$
$$C_{l1} = 1.89 + 0.0456\,(weight - 77) - 0.0681\,(lbm - 59) + 0.0264\,(height - 177)$$
$$C_{l2} = 1.29 - 0.024(age - 53), C_{l3} = 0.036$$

$$k_{10}=\frac{C_{l1}}{V_1}, k_{12}=\frac{C_{l2}}{V_1}, k_{13}=\frac{C_{l3}}{V_1}, k_{21}=\frac{C_{l2}}{V_2}, k_{31}=\frac{C_{l3}}{V_3} \quad (2)$$

Lean body mass for male and female are described in the following form, respectively:

$$lbm=1.1\,weight-128\,(\frac{weight}{height})^2 \quad (3)$$

$$lbm=1.07\,weight-148\,(\frac{weight}{height})^2 \quad (4)$$

As can be seen in (2), the values of $k_{10}, k_{12}, k_{13}, k_{21}$ and k_{31} depend on the *mass* (in kilogram), *height* (in centimeter), *age* (in years), and *gender* of the patients. V_1, V_2 and V_3 denote the central, second and third compartment's volume, respectively. The pharmacodynamics is related to the central compartment as:

$$\dot{C}_e(t)=k_{e0}(x_1(t)-C_e(t)) \quad (5)$$

where $k_{e0}=0.456\,s^{-1}$ and $C_e(t)$ is the effect-site compartment concentration. The relationship between BIS and the drug effect concentration can be described as follows [4]:

$$BIS=E_0-E_{\max}\,(C_e(t)^{\gamma}/(C_e(t)^{\gamma}+C_{50}{}^{\gamma})) \quad (6)$$

where E_0 denotes the awake state (without drug) value and $E_{\max}$ denotes the maximum effect achieved by the drug infusion, C_{50} is the drug concentration at half maximal effect and represents the patient's sensitivity to the drug, and γ determines the steepness of the curve in (6). With these equations the patient model is completed. Table 1 tabulates and lists the characteristics of the patients.

3. Controller design

3.1. Sliding mode control

Consider the following time-varying nonlinear system:

$$\ddot{x}(t)=f(X,t)+g(X,t)\,u_1(t)+d(t) \quad (7)$$

where $X=[x(t)\ \ \dot{x}(t)]^T$ is the system states vector, $f(X,t)$ and $g(X,t)$ are the unknown smooth functions, $u_1(t)$ is control input, and $d(t)$ is external disturbance. The main target of this controller is to design an adaptive fuzzy sliding mode controller to be robust versus inter-intra patient's variability and external disturbances, guarantees boundedness of all the variables of the closed-loop system, and accurate tracking of a given reference signal $x_d(t)$. In order to meet all above mentioned items, the sliding mode function is defined as follows:

$$s(t)=\dot{e}(t)+\lambda e(t) \quad (8)$$

where $e(t)$ is tracking error which can be defined as:

$$e(t)=x(t)-x_d(t) \quad (9)$$

From (8) when $s(t)\to 0$ it can be observed that $e(t)\to 0$ exponentially. By taking time derivative of the equation corresponding to the sliding mode function, we have:

$$\dot{s}(t) = \ddot{x}(t) - \ddot{x}_d(t) + \lambda \dot{e}(t) \tag{10}$$

Power rate reaching law is defined as:

$$\dot{s}(t) = -k \mid s \mid^{\alpha} \operatorname{sgn}(s) \tag{11}$$

By assuming that $g(X,t)$ is a nonsingular function and substituting the equations (10) and (11) in (7), we can get the sliding mode controller as:

$$u_1(t) = g^{-1}(X,t) \left[- f(X,t) + \ddot{x}_d(t) - \lambda \dot{e}(t) - k \mid s \mid^{\alpha} \operatorname{sgn}(s) \right] \tag{12}$$

The nonlinear dynamics $f(X,t)$ and $g(X,t)$ in (12) are unknown bounded functions.

3.2. Fuzzy approximation

In practical systems we may not know the exact mathematical model of the plant. Because of the ability of the fuzzy logic systems for description about the processes by using IF-THEN statement, in recent years fuzzy systems have stirred a great deal of interests. In this part, our goal is to approximate the unknown functions $f(X,t)$ and $g(X,t)$ by using a method which has been proposed in [22]:

$$y(x) = \frac{\sum_{k=1}^{N} \mu_k(x)\, d_k}{\sum_{k=1}^{N} \mu_k(x)} \tag{13}$$

where

$$\mu_k(x) = \prod_{i=1}^{n} \mu_{F_i^{ij}}(x_i) \tag{14}$$

where $\mu_{F_i^{ij}}(x_i)$ is the membership function of the fuzzy set F_i^{ij}, and d_k is the point at which the membership function of C^k achieves its maximum value. Using (13) and (14) we can rewrite the output of fuzzy system as follows:

$$y(x) = W^T(x)\,\theta \tag{15}$$

where $\theta = [d_1 \ldots d_k]^T$ is a vector including all consequent parameters, and $W(x) = [w_1(x) \ldots w_n(x)]^T$ is a set of fuzzy basis functions defined as:

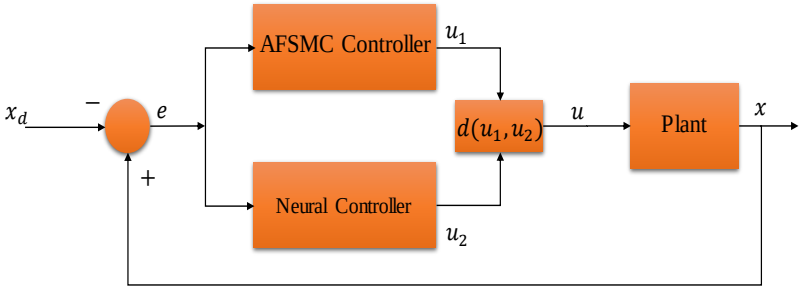

Figure 2: The structure of neural and AFSMC controller.

$$w_k(x)=\frac{\mu_k(x)}{\sum_{j=1}^{N}\mu_j(x)},\quad k=1,\ldots,n \tag{16}$$

Using (15) and (16) the system uncertainties in (12) can be approximated as follows:

$$\hat{f}(X,\theta_f)=W_f^T(X)\,\theta_f \tag{17}$$

$$\hat{g}(X,\theta_g)=W_g^T(X)\,\theta_g \tag{18}$$

where $W_f(X)$ and $W_g(X)$ are fuzzy basis vectors fixed by the designer. θ_f and θ_g are adjustable parameters. The adaptive laws for adaptation of these parameters can be written as follows:

$$\dot{\theta}_f=-\eta_f\,W_f(X)\,s,\qquad \eta_f>0 \tag{19}$$

$$\dot{\theta}_g=-\eta_g\,W_g(X)\,s\,u_1(t),\qquad \eta_g>0 \tag{20}$$

Now we can substitute the value of $\hat{f}(X,\theta_f)$ and $\hat{g}(X,\theta_g)$ in control law (12) as follows:

$$u_1(t)=\hat{g}^{-1}(X,t)\left[-\hat{f}(X,t)+\ddot{x}_d(t)-\lambda\,\dot{e}(t)-k\,|s|^{\alpha}\,\mathrm{sgn}(s)\right] \tag{21}$$

3.3. Neural control

In order to suppress chattering due to SMC we used neural control which has been proposed in [28]. At the beginning SMC forces the system state toward the sliding surface. When state trajectory of the system goes into the boundary layer, SMC is replaced by neural controller. The output of the neuron is given by:

$$u_2=h(net)=\alpha\frac{[1-\exp(-\beta\,net)]}{[1+\exp(-\beta\,net)]} \tag{22}$$

$$net=\varepsilon+\dot{\varepsilon}-\gamma \tag{23}$$

where $\varepsilon=x-x_d$ is threshold, and net denotes the neuron input. For the online adaption of the network parameter $\Gamma=[\alpha,\beta,\gamma]^T$, the following Lyapunov function can be defined as:

$$V=\frac{1}{2}\varepsilon^2 \tag{24}$$

The goal is to minimize (24) by online adaption of network parameter which can be achieved by using the following equation [28]:

$$\dot{\Gamma} = -\mu\, \varepsilon(t) \frac{\partial u_2}{\partial V} \operatorname{sgn} \frac{\partial x}{\partial u} \tag{25}$$

where $\mu > 0$ is learning parameter and $\operatorname{sgn}(.)$ is the sign function. Figure 2 shows the complete structure of AFSMC and neural controller, where u_1 is the output of AFSMC controller, u_2 is the output of neural controller, and $d(u_1,u_2)$ is a function of u_1 and u_2 defined by:

$$d(u_1,u_2) = \begin{cases} u_1, & |\, s(e)\,| > \phi + \xi \\ \alpha(e)\, u_1 + (1-\alpha(e))\, u_2, & \phi < |\, s(e)\,| \le \phi + \xi \\ u_2, & |\, s(e)\,| \le \phi \end{cases} \tag{26}$$

where ϕ and ξ are the boundary layer thicknesses, and $\alpha(e)$ is a function of error as follows:

$$\alpha(e) = \frac{|\, s(e)\,| - \phi}{\xi} \tag{27}$$

4. Results

In this section, we have presented the results for silico patients. Characteristic variables for all of eight patients have been shown in Table 1. Control performance of AFSMC strategy has been compared with fuzzy logic strategy in a way that both of controllers have been tuned for patient 1. The parameters of AFSMC are $\lambda = 4$ and $k = 150$, and the inputs of FLC are error and its derivative. This controller uses four rules which are tabulated in Table 2. The membership functions of linguistic variables Positive and Negative are S-shaped membership function and Z-shaped membership function, respectively. These membership functions are described in the following equations:

$$s(x;a,b) = \begin{cases} 0 & x \le a \\ 2\left(\frac{x-a}{b-a}\right)^2 & a < x \le \frac{a+b}{2} \\ 1 - 2\left(\frac{x-b}{b-a}\right)^2 & \frac{a+b}{2} < x \le b \\ 1 & b < x \end{cases} \tag{28}$$

$$z(x;a,b) = \begin{cases} 1 & x \le a \\ 1 - 2\left(\frac{x-a}{b-a}\right)^2 & a < x \le \frac{a+b}{2} \\ 2\left(\frac{x-b}{b-a}\right)^2 & \frac{a+b}{2} < x \le b \\ 0 & b < x \end{cases} \tag{29}$$

The membership functions of linguistic variables Small, Medium, Large, and Very Large are singleton which have been placed in 0, 0.2, 1, and 5, respectively. The fuzzifier is singleton and the defuzzifier is centroid. In evaluating the ANDs, and ORs in the fuzzy rules, the min fuzzy logic AND operator and max fuzzy logic OR operator are used, respectively. All the simulations have been performed in the MATLAB\Simulink. In this study, we have used some indexes to quantify the

controllers' performance, that are listed in Table 3. The values of indexes have been presented in Table 4. As we mentioned earlier, BIS is defined as controlled variable and the control input is the infusion rate of propofol. The results of closed-loop simulations for the controlled output (BIS) and control input (Propofol) with AFSMC and FLC strategies are shown in Figures 3 and 5, respectively. From these figures, it can be seen that the output of AFSMC controller reaches the set point faster than that of FLC, so the settling time is shorter and the steady state error for all patients is smaller. Therefore, AFSMC controller has appropriate performance in the reduction of settling time and steady state error point of view. However, in both controllers the control input is smooth without any oscillation, in fuzzy approach the amplitude of control input is very large compared to AFSMC strategy. Furthermore, these results reveal that with AFSMC strategy in all patients, the overdosing and underdosing do not exist, whereas in FLC it does not exist except for one patient. In addition, as the AFSMC strategy takes into account the patient variability, it obtains much better control performance and robustness. Figure 4 depicts the sliding variable. This figure shows the fact that the error signal converges to zero in finite time.

Table 1: Characteristic variables for each of the eight patients used in our study [4].

Patient	Age	Height	Weight	Sex	C50	E0	Emax	Gamma
1	40	163	54	F	6.33	98.8	94.1	2.24
2	36	163	50	F	6.76	98.6	86	4.29
3	28	164	52	F	8.44	91.2	80.7	4.10
4	50	163	83	F	6.44	95.9	102	2.18
5	28	164	60	M	4.93	94.7	85.3	2.46
6	43	163	59	F	12.1	90.2	147	2.42
7	37	187	75	M	8.02	92.0	104	2.10
8	38	174	80	F	6.56	95.5	76.4	2.12

Table 2: The rules of FLC.

e / $\dot{e}$	**Negative**	**Positive**
Negative	Very Small	Medium
Positive	Large	Small

onset of 10% during which continuous normal surgical stimulations might occur and during the skin-closing period, stimulus C simulates the withdrawal of stimulations. The results of the controller after applying this disturbance for all patients have been shown in Figure 7 in which top figure shows the value of BIS and the bottom figure indicates the control input. Considering these Figures, demonstrates that the system is robust against applying surgical stimulus. Considering these Figures, demonstrates that the system is robust against applying surgical stimulus.

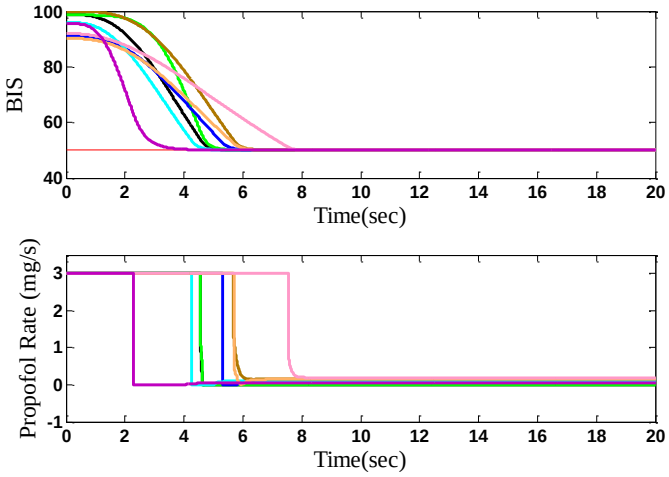

Figure 3: The results of closed-loop simulations for the controlled output (BIS) and control input (Propofol) with AFSMC strategy. Black for patient 1, green for patient 2, blue for patient 3, cyan for patient 4, brown for patient 5, orange for patient 6, pink for patient 7, purple for patient 8, and red solid line at the top figure for the target value.

Table 3: Indexes that are used to evaluate the controllers' performance.

Index	Description
TT	Observed time-to-target (in seconds) required for reaching first time the target interval of [55,45] BIS values [4].
BIS_NADIR	The lowest observed BIS value during induction phase [4].
ST	Settling time on the reference BIS value, defined within ± 5 BIS and stay within this BIS range [4].
US	Undershoot, defined as the BIS value that exceeds the limit of the defined BIS interval, namely, the 45 BIS value [4].
RMS	Root mean square of the error between desired and actual value of BIS.

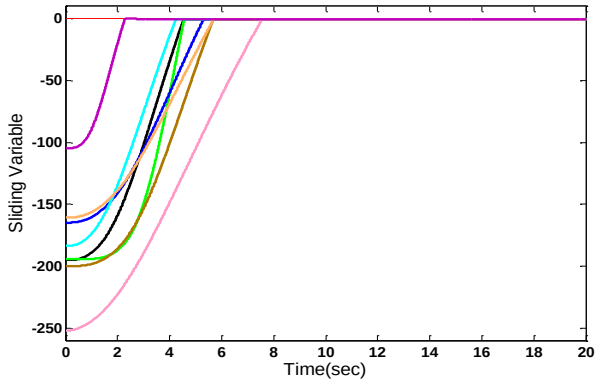

Figure 4: Sliding varible. The colors are the same as Fig. 3.

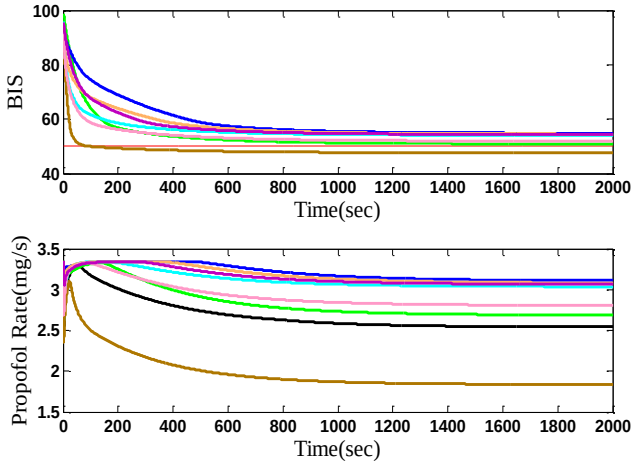

Figure 5: The results of closed-loop simulations for the controlled output (BIS) and control input (Propofol) with FLC strategy. The colors are the same as Figure 3.

Table 4. The value of indexes are used to evaluate the controllers' performance. See Table 3 for explanation.

Index	Method	P1	P2	P3	P4	P5	P6	P7	P8	Mean	STD
	FLC	130	290	1412	643	29	1042	294	831	583.8	**484.7**
1	**AFSMC**	4	4	5	4	5	5	6	2	4.4	**1.2**
	FLC	50	50	54.8	54.05	47.64	54.50	51.91	54.34	52.15	**2.68**
2	**AFSMC**	50	50	50	50	50	50	50	50	50	**0**
	FLC	1518	1801	2002	1724	1444	1935	1762	1783	1746.1	**188.82**
3	**AFSMC**	7	7	8	8	8	8	12	4	7.75	**2.18**
	FLC	0	0	0	0	0	0	0	0	0	**0**
4	**AFSMC**	0	0	0	0	0	0	0	0	0	**0**
	FLC	3.23	5.36	8.93	5.76	3.02	7.27	4.07	7.19	5.6	**2.1**
5	**AFSMC**	0.06	0.06	0.00	0.08	0.08	0.05	0.00	0.00	0.04	**0.03**

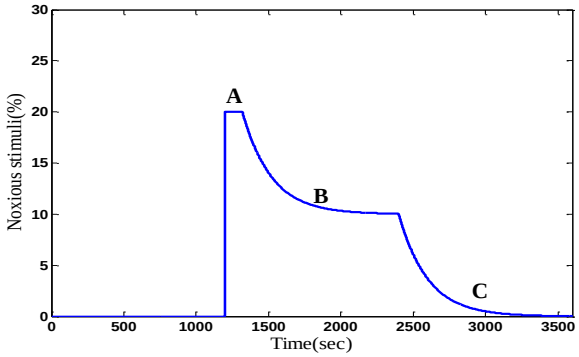

Figure 6: Surgical stimuli.

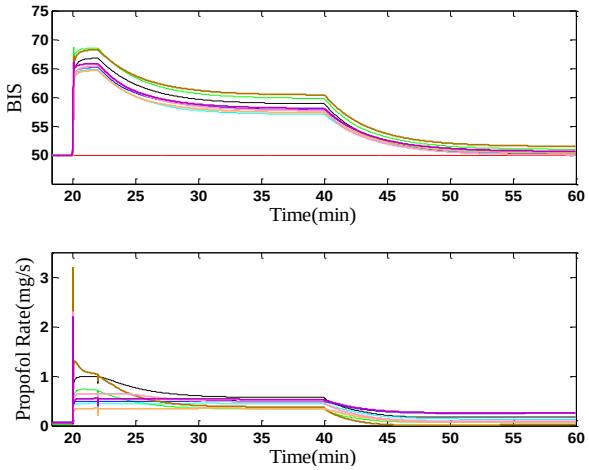

Figure 7: Closed-loop response of the BIS after applying surgical stimuli with AFSMC strategy. Top and bottom figures show the BIS and control input, respectively. The colors are the same as Figure 3.

Conclusion

In this study we proposed a new robust strategy which incorporates an auto-tuning neuron into the AFSMC for controlling the DOA. In this scheme, the stability study for online adaption of parameter is performed by using the Lyapunov stability theory so that boundedness of all the variables of the closed-loop system and accurate tracking of a given reference signal can be guaranteed. In our proposed strategy we have used power rate reaching law. Also, as we mentioned in section 3 we used the neural controller in order to chattering suppression. Previous studies in DOA control have some disadvantages such as improper performance in the presence of inter-intra patient's variability and disturbances, relatively large settling time, overdosing and underdosing which may cause pain and awareness during surgery and a delayed recovery, control input signal with intense switching action that causes low control accuracy, high wear of moving mechanical parts, high-heat losses in power circuits, and can excite unmodeled and high frequency dynamics. Main contribution of the present study is improvement of aforementioned deficiencies. Extensive simulation studies on 8 patients indicated the exceptional performance and robustness of the AFSMC versus inter-intra patient's variability and disturbance. The results show that the average settling time achieved using our proposed method is 7.75 ± 2.16 which is significantly shorter than that achieved with control strategy proposed in [4], [30] (122.91 ± 41.85). Also, there are other indexes in Table 3, the values of these indexes are presented in Table 4. Compared to [4], [30], the values of other indexes was further improved with the use of AFSMC. Our method resulted in small RMS error and fast convergence. The fast convergence is the direct outcome of the power rate reaching law. This is because it increases the reaching speed when the state is far away from the switching manifold. However, it reduces the rate when the state is near the manifold. The result is a fast and low chattering reaching mode.

Appendix A

Consider the following Lyapunov function candidate:

$$V = \frac{1}{2}(s^2 + \frac{1}{\eta_f}\tilde{\theta}_f^T\,\tilde{\theta}_f + \frac{1}{\eta_g}\tilde{\theta}_g^T\,\tilde{\theta}_g) \tag{A.1}$$

Estimation error, and θ_f^* and θ_g^* are the optimum parameter of fuzzy approximator. We can write the time derivative of (A.1) as following form:

$$\dot{V} = s\,\dot{s} + \frac{1}{\eta_f}\tilde{\theta}_f^T\,\dot{\tilde{\theta}}_f + \frac{1}{\eta_g}\tilde{\theta}_g^T\,\dot{\tilde{\theta}}_g \tag{A.2}$$

The time derivative of (8) can be written as follows:

$$\dot{s} = \ddot{e} + \lambda\,\dot{e} = \ddot{x}(t) - \ddot{x}_d(t) + \lambda\,\dot{e}(t) \tag{A.3}$$

Substituting (7) into (A.3) we have:

$$\begin{aligned}\dot{s} = {} & f(X,t) + g(X,t)\,u_1(t) + d(t) - \hat{g}(X\,|\,\theta_g)\,u_1(t) \\ & - \hat{f}(X\,|\,\theta_f) - k\,|\,s\,|^{\alpha}\,\mathrm{sgn}(s)\end{aligned} \tag{A.4}$$

We can define the following equations:

$$f(X,t) - \hat{f}(X\,|\,\theta_f) = \hat{f}(X\,|\,\theta_f^*) - \hat{f}(X\,|\,\theta_f) + \varepsilon_f(X) \tag{A.5}$$

$$g(X,t) - \hat{g}(X\,|\,\theta_f) = \hat{g}(X\,|\,\theta_g^*) - \hat{g}(X\,|\,\theta_g) + \varepsilon_g(X) \tag{A.6}$$

Substituting (A.5) and (A.6) into (A.4) we have:

$$\begin{aligned}\dot{s} = {} & \hat{f}(x\,|\,\theta_f^*) - \hat{f}(x\,|\,\theta_f) + \varepsilon_f(x) + d(t) \\ & + (\hat{g}(x\,|\,\theta_g^*) - \hat{g}(x\,|\,\theta_g))\,u_1(t) \\ & + \varepsilon_g(x)\,u_1(t) - k\,|\,s\,|^{\alpha}\,\mathrm{sgn}(s)\end{aligned} \tag{A.7}$$

Now we can rewrite (A.4) as following form:

$$\begin{aligned}\dot{s} = {} & \tilde{\theta}_f^T\,W_f(x) + d(t) + \tilde{\theta}_g^T\,W_g(x)\,u_1(t) \\ & - k\,|\,s\,|^{\alpha}\,\mathrm{sgn}(s) + \xi\end{aligned} \tag{A.8}$$

where $\xi = \varepsilon_g(X)\,u_1(t) + \varepsilon_f(X)$. Substituting (A.8) into (A.2), we have:

$$\begin{aligned}\dot{V} = {} & s(\tilde{\theta}_f^T\,W_f(X) + \tilde{\theta}_g^T\,W_g(X)\,u_1(t) + d(t) \\ & - k\,|\,s\,|^{\alpha}\,\mathrm{sgn}(s) + \xi) + \frac{1}{\eta_f}\tilde{\theta}_f^T\,\dot{\tilde{\theta}}_f + \frac{1}{\eta_g}\tilde{\theta}_g^T\,\dot{\tilde{\theta}}_g \\ = {} & \tilde{\theta}_f^T\,(W_f(x)\,s + \frac{1}{\eta_f}\dot{\tilde{\theta}}_f) + \tilde{\theta}_g^T\,(W_g(X)\,s\,u_1(t) + \frac{1}{\eta_g}\dot{\tilde{\theta}}_g) \\ & + s\,(d(t) - k\,|\,s\,|^{\alpha}\,\mathrm{sgn}(s) + \xi)\end{aligned} \tag{A.9}$$

where $\dot{\tilde{\theta}}_f = \dot{\theta}_f$ and $\dot{\tilde{\theta}}_g = \dot{\theta}_g$. Therefore we have the following equation:

$$\dot{V} = -s\,(k\,|\,s\,|^{\alpha}\ \mathrm{sgn}(s) - \xi - d(t)) \tag{A.10}$$

In (A.10) we can see that $\dot{V} < 0$ if $k > \xi + D$. This completes the proof.

References

[1] Q. Labbaf, M. Aliyari, and M. Teshnehlab, "A new approach in drug delivery control in anesthesia," IEEE International Conference on Systems Man and Cybernetics, pp. 2064-2068, 2010.

[2] C. S. Nunes, T. F. Mendonca, P. Amorim, D. A. Ferreira, and L. Antunes, "Comparison of neural networks, fuzzy and stochastic prediction models for return of consciousness after general anesthesia," Proc. 44th IEEE Conf. on Decision & Control & European Control, pp. 4827-4832, 2005.

[3] A. Bamdadian, F. Towhidkhah, and M. H. Moradi, "Generalized predictive control of depth of anesthesia by using a pharmocokinetic-pharmacodynamic model of the patient," The 2nd ICBBE, pp. 1276-1279, 2008.

[4] C. M. Ionescu, R. De Keyser, B. C. Torrico, T. De Smet, M. M. Struys, and J. E. Normey-Rico, "Robust predictive control strategy applied for propofol dosing using BIS as a controlled variable during anesthesia," IEEE Trans. on Biomedical Engineering, vol. 55, no. 9, pp. 2161-2170, September 2008.

[5] M. Mahfouf, A. J. Asbury, and D. A. Linkens, "Unconstrained and constrained generalised predictive control of depth of anaesthesia during surgery," Control Engineering Practice, vol. 11, no. 12, pp. 1501-1515, December 2003.

[6] J. M. Bailey, and W. M. Haddad, "Drug dosing control in clinical pharmacology", IEEE Control System Magazine, vol. 25, no. 2, pp. 35-51, April 2005.

[7] S. Rezvanian, F. Towhidkhah, and N. Ghahramani, "Controlling the depth of anesthesia using model predictive controller and extended kalman filter," The 1st MECBME, pp. 213-216, 2011.

[8] S. Bibian, "Automation in clinical anesthesia", PHD Thesis, University of British Columbia, 2006.

[9] K. Ejaz, and J. S. Yang, "Controlling the depth of anesthesia using PID tuning: A comparative model-based study," Proc. IEEE, International Conf. on control application, pp. 580-585, 2004.

[10] J. S. Shieh, and M. H. Kao, C.C. Liu, "Genetic fuzzy modelling & control of bispectral index (BIS) for general intravenous anaesthesia", Medical Engineering & Physics, vol. 28, no. 2, pp. 134-148, March 2006.

[11] M. Elkfafi, J. S. Shieh, D. A. Linkens, and J. E. Peacock, "Fuzzy logic for auditory evoked response monitoring and control of depth of anesthesia, " Fuzzy sets and systems, vol. 100, no. 1-3, pp. 29-43, November 1998.

[12] J. S. Shieh, D. A. Linkens, and A. J. Asbury, "A hierarchical system of on-line advisory for monitoring and controlling the depth of anesthesia using self-organizing fuzzy logic", Artificial Intelligence, vol. 18, no. 3, pp. 307-316, April 2005.

[13] M. Delshad, "Improved the robustness and performance of a buck-boost type DC-DC convertor by using fuzzy sliding mode controller," International Journal of Mechatronics, Electrical and Computer Technology, vol.4, no. 13, pp. 1436-1451, October 2014.

[14] H. Sadegh and N. Bigdeli, "Multi-Surface sliding mode controller for stabilizing uncertain disturbed fractional-order chaotic systems," International Journal of Mechatronics, Electrical and Computer Technology, vol. 4, no. 11, pp. 693-708, April 2014.

[15] H. Nejatbakhsh, M. R. Sajadi, "Improved sliding mode control of a class of nonlinear systems: application to quadruple tanks system," International Journal of Mechatronics, Electrical and Computer Technology, vol. 3, no. 8, pp. 102-118, July 2013.

[16] K. van Heusden, G. A. Dumont, K. Soltesz, C. L. Petersen, A. Umedaly, N. West, and J. M. Ansermino, "Design and clinical evaluation of robust PID control of propofol anesthesia in children," IEEE Trans. on Control Systems Technology, vol. 22, no. 2, pp. 491-501, March 2014.

[17] S. Abdulla, and W. Peng, "Depth of anaesthesia control investigation using robust deadbeat control technique," ICME, pp. 107-111, 2012.

[18] Y. Tao, M. Fang, and Y. Wang, "A fault tolerant closed-loop anesthesia system based on internal model control and extended state observer," The 25th CCDC, pp. 4910-4914, 2013.

[19] A. Marrero, J. A. Mendez, A. V. Maslov, and M. Pechenizkiy, "ACLAC: An approach for adaptive closed-loop anesthesia control," The 26th IEEE symp. on CBMS, pp. 285-290, 2013.

[20] D. V. Caiado, J. M. Lemos, B. A. Costa, M. M. Silva, and T. F. Mendoca, "Design of depth of anesthesia controllers in the presence of model uncertainty," The 21st Mediterranean Conference on Control & Automation (MED), pp. 213-218, 2013.

[21] A. G. Hernandez, J. E. Escobar, R. Leder, A. L. Perez, L. Fridman, J. Davila, C. R. Monsalve, and S. I. Andrade, "High-order sliding-mode control for anesthesia," The 35th EMBC, pp. 201-204, 2013.

[22] S. Labioda, M. S. Boucheritb, and T. M. Guerrac, "Adaptive fuzzy control of a class of MIMO nonlinear systems," Fuzzy Sets and Systems, vol. 151, no. 1, pp. 59-77, April 2005.

[23] S. Tong and H. Li, "Fuzzy adaptive sliding-mode control for MIMO nonlinear systems," IEEE Trans. Fuzzy Syst., vol. 11, no. 3, pp. 354-360, June 2003.

[24] X. Lu and S. Spurgeon, "Robust sliding mode control of uncertain nonlinear systems," Systems & Control Letters, vol. 32, no. 2, pp. 75-90, November 1997.
[25] Y. Guo and P. Woo, "An adaptive fuzzy sliding mode controller for robotic manipulators," IEEE Trans. Syst., Man, Cybern.,Syst., vol. 33, no. 2, pp. 149-159, March 2003.
[26] Y. Hsu, G. Chen, and H. Li, "A fuzzy adaptive variable structure controller with applications to robot manipulators," IEEE Trans. Syst., Man, Cybern.,Syst., vol. 31, no. 3, pp. 331-340, June 2001.
[27] C. Hwang, "A novel takagi–sugeno-based robust adaptive fuzzy sliding-mode controller," IEEE Trans. Fuzzy Syst., vol. 12, no. 5, pp. 676-687, October 2004.
[28] W. Chang, R. Hwang, and J. Hsieh, "Application of an auto-tuning neuron to sliding mode control," IEEE Trans. Syst., Man, Cybern.,Syst., vol. 32, no. 4, pp. 517-522, November 2002.
[29] T. Schnider, C. Minto, P. Gambus, C. Andresen, D. Goodale, S. Shafer, E. Youngs, "The influence of method of administration and covariates on the pharmacokinetics of propofol in adult volunteers," The Journal of American Society of Anesthesiologists, vol. 88, no. 5, pp. 1170-1182, May 1998.
[30] G. Dumont, A. Martinez, and J. Mark, "Robust control of depth of anesthesia," International Journal of Adaptive Control and Signal Processing, vol. 23, no. 5, pp. 435-454, November 2008.